

New Organic Dyes Based on Diarylmethylene-Bridged Triphenylamine for Dye Sensitized Solar Cell

Fei Wu,^a Haitao Liu,^a Lawrence Tien Lin Lee,^b Tao Chen,^b Min Wang,^a and Linna Zhu^{*a}

^a Faculty of Materials and Energy, Southwest University, Chongqing 400715, China

^b Department of Physics, The Chinese University of Hong Kong, Shatin, New Territories, Hong Kong, China

Three new organic dyes were synthesized and characterized for applications in dye-sensitized solar cells (DSSCs). In these dyes, diarylmethylene-bridged triphenylamine is the donor, and different acceptors and vinyl-thiophene are designed to get TBA-1, TBA-2 and TBA-3. Their photophysical, electrochemical and photovoltaic properties were investigated, and the effects of the acceptor structures as well as the linkage on these properties were evaluated. Results demonstrated that the vinylthiophene linkage between the donor and the acceptor is favorable for improving light harvesting ability of TBA-2. In addition, the electrochemical impedance spectroscopy experiments suggest larger R_{rec} and longer electron lifetime of TBA-2. Therefore, it outperforms the other dyes, exhibiting the highest power conversion efficiency of 3.87%, with J_{sc} of $8.25 \text{ mA} \cdot \text{cm}^{-2}$ and V_{oc} of 666 mV. Unfortunately, the TBA-3 with three acceptor groups only shows efficiency of 3.52%, indicating that the design of increasing acceptor groups plays little role on enhancing the solar cell efficiency.

Keywords diarylmethylene-bridged triphenylamine, dye-sensitized solar cells, acceptor, rhodanine-3-acetic acid

Introduction

The interest in dye-sensitized solar cells (DSSCs) utilizing nanostructured TiO_2 semiconductor has increased enormously since the report by O'Regan and Grätzel in the 1990's.^[1] Compared to the inorganic silicon-based solar cells, DSSCs have advantages such as low costs and facile fabrication.^[2] In recent years, great efforts concerning the semiconductors, counter electrodes, electrolytes and sensitizers have been devoted to improving the power conversion efficiency. Among the components of DSSCs, the sensitizer plays a critical role in their performance and remains one of the most studied areas in the past two decades.^[3,4] Despite of their leading performance of polypyridyl Ru complexes and metalloporphyrins, metal-free organic dyes have become increasingly attractive owing to the following features: low-cost, high molar extinction coefficients, easy tuning of photophysical and electrochemical properties through molecular design.^[5-8] In recent years, enormous efforts have been dedicated to developing efficient organic dyes for DSSCs, and great achievements have been achieved.^[9]

Most of the organic sensitizers in highly efficient DSSCs are composed of donor (D) and acceptor (A) moieties connected by a π -conjugated spacer (D- π -A). The push-pull structure is very popular, since it can offer efficient intramolecular charge transfer (ICT) in the

excited state.^[10,11] Triphenylamine (TPA) is a widely used donor in DSSCs, and many organic dyes containing TPA have been designed and considerable efficiencies are achieved.^[12-16] In recent years, modification of the TPA structure has been conducted to further fine-tune the physical and optical properties of the sensitizers. For example, the introduction of alkoxy and aromatic groups to TPA has been reported to increase the HOMO energy level and increase the light harvesting ability of the dye molecules.^[17] Compared to the conventional TPA structure, bridged TPA shows better planarity of its core structure.^[18] With two adjacent phenyl rings connected by a substituted methylene, it has more extended conjugation and better electron delocalization. When functionalized with bulky substituents, the charge-separated state lifetime could be increased and dye aggregation could be inhibited.^[19,20] Initially, bridged triphenylamine derivatives were designed as efficient blue emitting materials in organic light emitting diodes (OLEDs).^[21] Only quite recently, bridged TPAs modified with *t*-butyl and dimethyl groups were utilized as the donor moieties for metal-free organic sensitizers respectively, and high power conversion efficiencies over 8% were achieved in both kinds of materials.^[22,23] Nevertheless, the investigation of bridged TPA in photovoltaics is still in its infancy to date.

Quite recently, we have reported the diarylmethylene-bridged TPA based dyes TB-1—TB-3 as sensitizers

* linzhu@swu.edu.cn; Tel.: 0086-023-68254957

Received February 14, 2015; accepted April 7, 2015; published online XXXX, 2015.

Supporting information for this article is available on the WWW under <http://dx.doi.org/10.1002/cjoc.201500137> or from the author.

for DSSCs. These dyes showed enhanced power conversion efficiencies (~21% increase) compared to their triphenylamine counterpart, suggesting rational choice of the planar donor structure.^[24] Therefore, in this article, we further present the design and synthesis of three new organic dyes based on diarylmethylene-bridged TPA, namely TBA-1, TBA-2, and TBA-3. In the newly designed dyes, thiophene is used as the π -spacer, and different acceptors and linkages are incorporated to investigate how the structure changes affect the solar cell performance. In model compound TB-1, the bridged TPA donor is connected to the cyanoacrylic acceptor through a thiophene spacer. In TBA-1, rhodanine-3-acetic acid is the electron acceptor (meanwhile the anchoring group), which is directly linked to the thiophene spacer. In TBA-2, the thiophene spacer is connected to the cyanoacrylic acid acceptor by the vinyl linkage. While in TBA-3, three cyanoacrylic acid groups are attached on the TPA framework through the thiophene spacer. Their chemical structures are shown in Scheme 1. Dye TB-1 with one cyanoacrylic acid group was also presented for comparison. We attempt to investigate the influence of the acceptor structures and the way of linkage toward the solar cell performance. Toluene groups on the periphery of TPA core could avoid intermolecular aggregation, and meanwhile increase the dye solubility. The novel bridged triphenylamine-based sensitizers are applied as sensitizers and the corresponding photophysical and photovoltaic properties are discussed

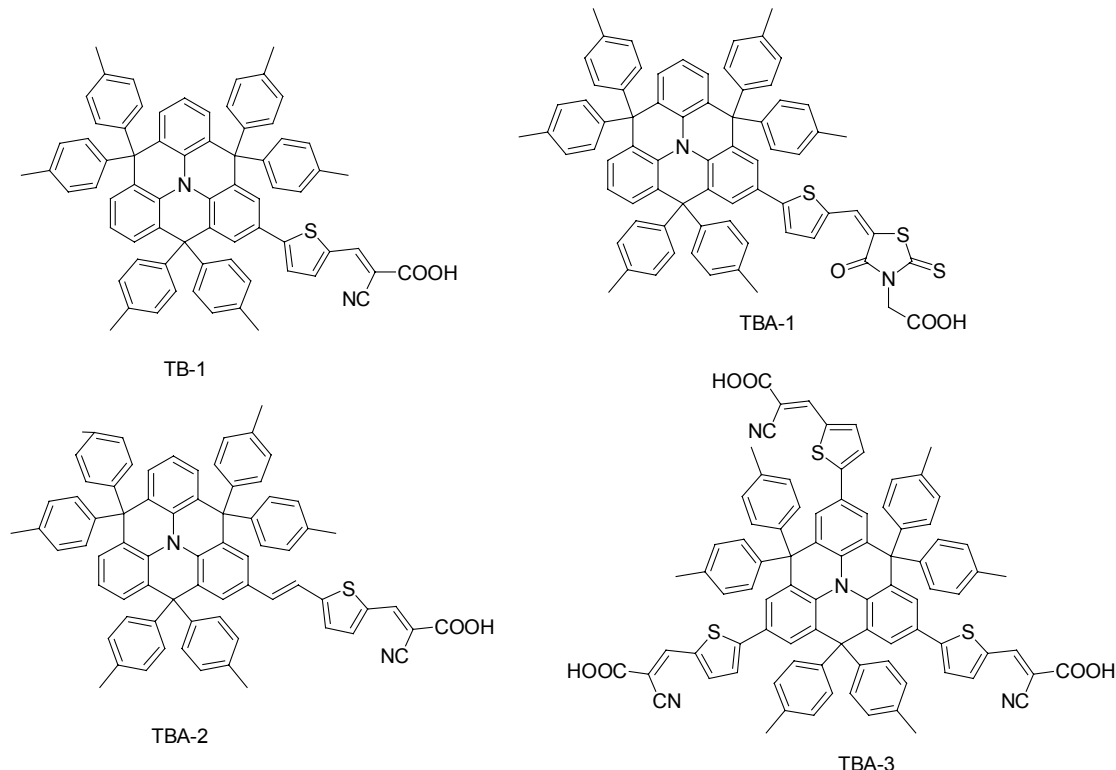
in the present work.

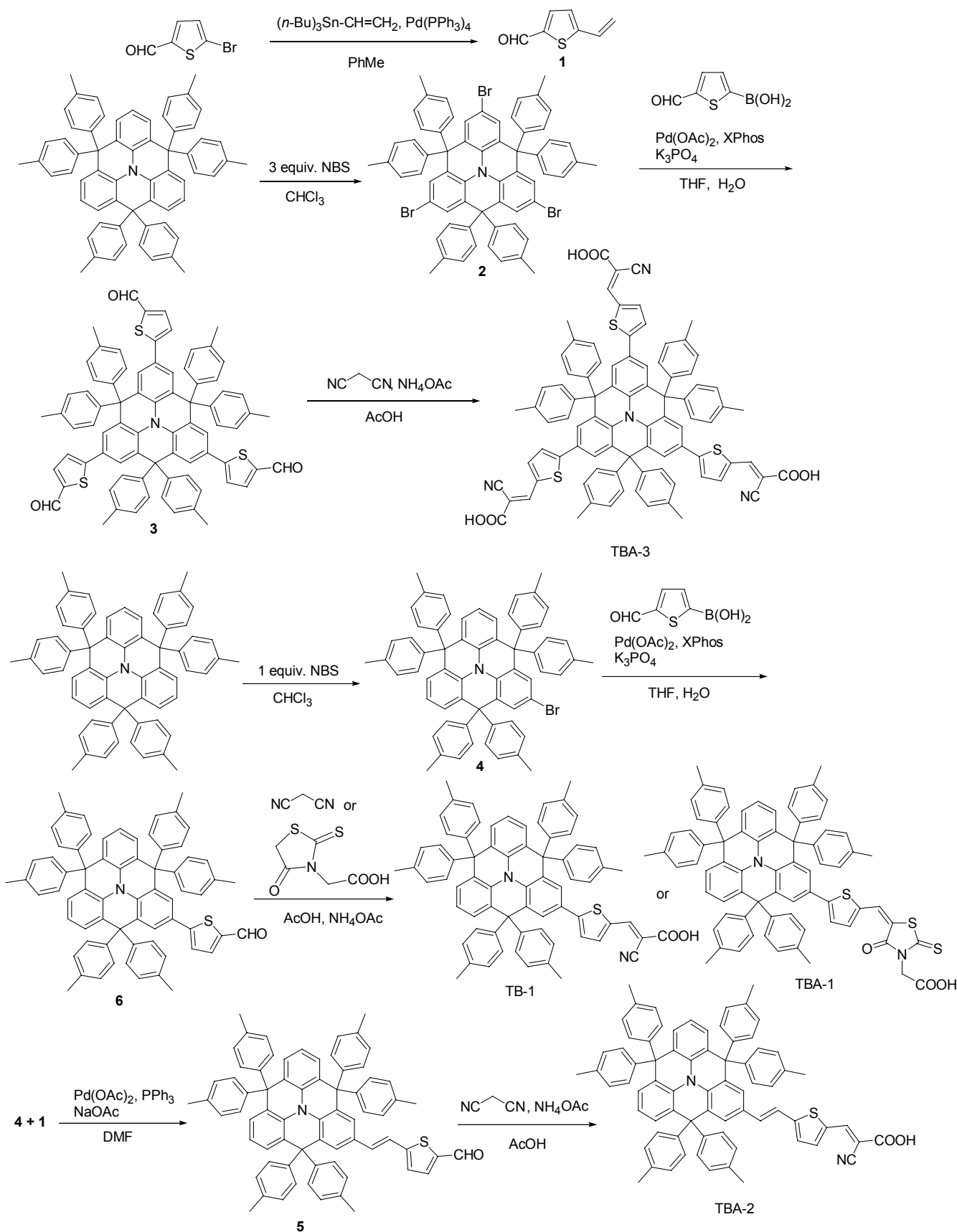
Experimental

The ^1H NMR and ^{13}C NMR spectra were recorded on a BRUKER AVANCE III 600 MHz NMR instrument in CDCl_3 and $\text{DMSO}-d_6$, using tetramethylsilane as an internal reference. LC-Ms was recorded on a GCMS-QP2010 Plus Spectrometer. MALDI-TOF was performed on a Bruker Autoflex instrument, using 1,8,9-trihydroxyanthracene as a matrix. Elemental analyses of carbon, hydrogen, and nitrogen were performed on a Carlorerba-1106 microanalyzer. The HRMS was measured on Thermo Scientific Q Exactive instrument. UV-Vis absorption spectra were recorded on a spectrophotometer (UV-2450, Shimadzu). Electrochemical experiments were performed using a CH Instruments electrochemical workstation (model 660A). The experiments were carried out in CH_2Cl_2 solution under Ar atmosphere with tetrabutylammonium hexafluorophosphate ($n\text{-Bu}_4\text{NPF}_6$) as a supporting electrolyte at a scan rate of $50 \text{ mV}\cdot\text{s}^{-1}$. The potentials are quoted against the ferrocene internal standard.

All starting materials were purchased from commercial suppliers (Sigma-Aldrich, J&K Scientific, and Energy Chemical) and used without further purification. Tetrahydrofuran (THF) for synthesis was freshly distilled over Na-K alloy under argon atmosphere prior to use. The general synthetic routes for the intermediates

Scheme 1 Chemical structures of new bridged TPA based dyes TBA-1, TBA-2, TBA-3 and TB-1



Scheme 2 Synthetic procedures for bridged TPA based dyes TBA-1, TBA-2 and TBA-3

and the final compounds are outlined in Scheme 2. 5-Vinylthiophene-2-carbaldehyde (**1**),^[19] the intermedi-

ates **2**^[21] and **4**^[25] were synthesized as described in the literature. The intermediate **3** was synthesized by palladium-catalyzed Suzuki coupling reaction of 5-formyl-2-thiophene-boronic acid and the corresponding substrates. The intermediate **5** was synthesized by palladium-catalyzed Heck coupling reaction of compound **4** and 5-vinylthiophene-2-carbaldehyde (compound **1**). The syntheses of TB-1 and intermediate compound **4** and compound **6** have been reported in our other work.^[24] The final compounds were synthesized in a similar way to literature report.^[26,27] The final products were fully characterized by ¹H NMR spectroscopy, MALDI-TOF spectrometry, the elemental analysis and the high resolution mass spectra as well. Unfortunately, the ¹³C NMR spectra of the final products were not able to be obtained due to their poor solubility.

Compound 3

A mixture of compound **2** (212 mg, 0.2 mmol), 5-formyl-2-thiophene-boronic acid (109 mg, 0.7 mmol), Pd(OAc)₂ (2.2 mg, 0.01 mmol), xphos (5.7 mg, 0.012 mmol) and aqueous solution of K₃PO₄ (2 mol/L, 3 mL) in tetrahydrofuran (10 mL) was placed in a Schlenk tube under an argon atmosphere and stirred at 60 °C for 12 h. After cooling, the reaction was quenched by adding water, and then was extracted with chloroform. The organic layer was washed with brine and dried over anhydrous Na₂SO₄. After evaporation of solvents, the residue was purified by column chromatography over silica gel using hexane/chloroform mixture (2 : 5) as the eluent to give the product (159 mg, 69%) as a yellow solid. ¹H NMR (600 MHz, CDCl₃) δ: 9.77 (s, 3H, CHO), 7.57 (d, J=4.2 Hz, 3H), 7.16 (dd, J=27.1, 2.2 Hz, 6H), 6.92 (d, J=4.2 Hz, 3H), 6.88 (d, J=8.4 Hz, 12H), 6.65 (d, J=8.4 Hz, 6H), 6.61 (d, J=8.4 Hz, 6H), 2.32 (t, J=6.9 Hz, 18 H); ¹³C NMR (150 MHz, CDCl₃) δ: 182.51, 154.21, 141.97, 141.80, 141.73, 137.62, 136.05, 135.52, 133.72, 131.08, 130.69, 129.89, 129.66, 128.56, 127.60, 125.90, 123.16, 116.38, 55.28, 20.97. Anal. calcd for C₇₈H₅₇N₁O₃S₃: C 81.29, H 4.99, N 1.22; found C 81.64, H 4.79, N 1.34; MALDITOF-MS m/z: 1152.1 (M⁺).

Compound 5

A mixture of compound **4** (450 mg, 0.5 mmol), 5-vinylthiophene-2-carbaldehyde (69 mg, 0.5 mmol), Pd(OAc)₂ (2.2 mg, 0.01 mmol), PPh₃ (5.7 mg, 0.012 mmol), TBAB (4.8 mg, 0.015 mmol) and NaOAc (205 mg, 2.5 mmol) in DMF (15 mL) was placed in a Schlenk tube under an argon atmosphere and stirred at 110 °C for 2 d. After cooling, the reaction was quenched by adding water, and then was extracted with chloroform. The organic layer was washed with brine and dried over anhydrous Na₂SO₄. After evaporation of solvents, the residue was purified by column chromatography over silica gel using hexane/chloroform mixture (1 : 2) as the eluent to give the product (230 mg, 48%) as a pale red solid. ¹H NMR (600 MHz, CDCl₃) δ: 9.67 (s, 1H, CHO), 7.49 (d, J=3.6 Hz, 2H), 7.16 (s, 2H),

6.96–6.92 (m, 6H), 6.89 (d, J=3.6 Hz, 2H), 6.82 (d, J=7.8 Hz, 12 H), 6.58 (d, J=7.8 Hz, 12 H), 2.33 (s, 18H); ¹³C NMR (150 MHz, CDCl₃) δ: 181.34, 152.78, 142.14, 141.89, 140.35, 136.56, 136.02, 135.36, 135.12, 134.57, 133.46, 130.68, 130.39, 130.12, 129.98, 129.74, 129.48, 129.06, 128.57, 128.42, 128.29, 128.22, 128.15, 128.10, 126.57, 125.41, 122.82, 55.24, 55.17, 29.72, 20.96, 20.87. Anal. calcd for C₇₀H₅₅NOS: C 87.74, H 5.79, N 1.46; found C 87.81, H 5.68, N 1.54; MALDI-TOF-MS m/z: 958.7 (M⁺).

Compound TBA-1

A mixture of compound **7** (140 mg, 0.15 mmol), rhodanine-3-acetic acid (86 mg, 0.45 mmol), ammonium acetate (56 mg, 0.74 mmol), and acetic acid (20 mL) was heated at reflux for 6 h under argon atmosphere. After cooling to room temperature, it was precipitated by pouring into water. The resulting solid was filtered, washed thoroughly with water. Then, the crude product was purified by silica-gel column chromatography using chloroform/ethanol mixture (7 : 1) as the eluent to afford TBA-1 as a deep red solid (119 mg, 72%). ¹H NMR (600 MHz, CDCl₃) δ: 8.02 (br, 1H), 7.74 (br, 1H), 7.60 (br, 2H), 7.52 (br, 1H), 7.16–7.06 (m, 4H), 6.96–6.94 (m, 2H), 6.90–6.83 (m, 12H), 6.64–6.57 (m, 10H), 6.46 (d, J=7.8 Hz, 2H), 4.80 (s, 2H, CH₂COOH), 2.28 (s, 18H). Anal. calcd for C₇₃H₅₆N₂O₃S₃: C 79.32, H 5.11, N 2.53; found C 79.80, H 4.73, N 2.89; MALDITOF-MS m/z: 1104.3 (M⁺). HRMS-ESI m/z: calcd for C₇₃H₅₆N₂O₃S₃ ([M]⁺) 1103.3380, found 1103.3387.

Compound TBA-2

A mixture of compound **6** (144 mg, 0.15 mmol), cyanoacetic acid (38 mg, 0.45 mmol), ammonium acetate (56 mg, 0.74 mmol), and acetic acid (20 mL) was heated at reflux for 6 h under argon atmosphere. After cooling to room temperature, it was precipitated by pouring into water. The resulting solid was filtered, washed thoroughly with water. Then, the crude product was purified by silica-gel column chromatography using chloroform/ethanol mixture (5 : 1) as the eluent to afford TBA-3 as a deep red solid (103 mg, 70 %). ¹H NMR (600 MHz, CDCl₃) δ: 8.20 (s, 1H, CH=C), 7.46 (br, 2H), 7.08–7.03 (m, 2H), 7.00–6.93 (m, 4H), 6.86–6.84 (m, 12H), 6.78 (d, J=7.2 Hz, 4H), 6.66–6.62 (m, 12H), 2.29 (s, 18H). Anal. calcd for C₇₃H₅₆N₂O₂S: C 85.51, H 5.51, N 2.73; found C 85.69, H 5.31, N 2.83; MALDITOF-MS m/z: 1024.4 (M⁺–1). HRMS-ESI m/z: calcd for C₇₃H₅₆N₂O₂S ([M]⁺) 1023.3990, found 1023.3997.

Compound TBA-3

A mixture of compound **4** (173 mg, 0.15 mmol), cyanoacetic acid (76 mg, 0.90 mmol), ammonium acetate (112 mg, 1.48 mmol), and acetic acid (20 mL) was heated at reflux for 6 h under argon atmosphere. After cooling to room temperature, it was precipitated by

pouring into water. The resulting solid was filtered, washed thoroughly with water. Then, the crude product was purified by silica-gel column chromatography using chloroform/ethanol mixture (7 : 2) as the eluent to afford TBA-4 as a deep red solid (134 mg, 66%). ¹H NMR (600 MHz, CDCl₃) δ: 8.18 (s, 3H, CH=C), 7.74 (d, *J*=4.2 Hz, 3H), 7.21 (d, *J*=2.4 Hz, 2H), 7.10 (d, *J*=1.8 Hz, 2H), 7.07 (s, 2H), 6.98 (d, *J*=4.2 Hz, 3H), 6.92–6.88 (m, 12H), 6.66 (d, *J*=7.8 Hz, 4H), 6.61 (d, *J*=7.8 Hz, 8H), 2.34 (s, 6H), 2.32 (s, 12H). Anal. calcd for C₈₇H₆₀N₄O₆S₃: C 77.19, H 4.47, N 4.14; found C 77.35, H 4.08, N 4.41; MALDITOF-MS *m/z*: 1353.4 (M⁺). HRMS-ESI *m/z*: calcd for C₈₇H₆₀N₄O₆S₃ ([M]⁺) 1351.3602, found 1351.3607.

Fabrication and characterization of DSSCs

All of the anode films for the DSSCs were made under the same standard condition,^[28] which are composed of a 12 μm thick transparent layer (TiO₂ with diameter of 20 nm) and a 6 μm thick scattering layer (TiO₂ nanoparticles with diameter of 200 nm). The electrodes were immersed into a 0.3 mmol/L dye bath in THF/EtOH (volume ratio, 1 : 1) solution for the bridged triphenylamine dyes (TBA-1–TBA-3), and were maintained in the dark for 18 h. Then, the electrodes were rinsed with ethanol to remove the non-adsorbed dyes and dried in the air. Pt counter electrodes were prepared by sputtering method at 13 mA for 180 s at a power of 150 W. The liquid electrolyte consisting of 0.6 mol/L 1,2-dimethyl-3-propylimidazolium iodide (DMPII), 0.1 mol/L LiI, 0.05 mol/L I₂ in a mixture of acetonitrile and 4-*tert*-butylpyridine (volume ratio, 1 : 1) was introduced into the cell through the drilled holes at the back of the counter electrode. The effective areas of all the TiO₂ electrodes were 0.196 cm². The current-voltage (*J-V*) characteristics of the assembled DSSCs were measured by a semiconductor characterization system (Keithley 236) at room temperature in air under the spectral output from solar simulator (Newport) using an AM 1.5G filter with a light power of 100 mW/cm². IPCEs of DSSCs were recorded in the Solar Cell QE/IPCE Measurement System (Zolix Solar Cell Scan 100) using DC mode. CHI 760E electrochemical workstation was used to characterize the electrochemical properties of the DSSCs. Electrochemical impedance spectroscopy (EIS) was recorded under dark conditions over a frequency range of 0.1–10⁵ Hz with an AC amplitude of 10 mV, and the parameters were calculated from Z-View software (v2.1b, Scribner AssociaNe, Inc.). For the open-circuit voltage decay measurements, the cell was first illuminated for 20 s to a steady voltage, then the illumination was turned off for 80 s and the open-circuit voltage decay curve was recorded.

Results and Discussion

The UV-Vis absorption spectra of the dyes in chloroform (*ca.* 10⁻⁶ mol/L) are depicted in Figure 1. Gen-

erally, in these dyes, two absorption bands could be observed. The one below 400 nm is ascribed to the π-π* transition of the bridged TPA, and the one located at longer wavelength (around 500 nm) is assigned to the intramolecular charge transfer (ICT) band from bridged TPA to the corresponding acceptors. The λ_{max} for TBA-1 has prominent red shift compared to the other dyes, but with quite low absorption intensity. As summarized in Table 1, the λ_{max} s appear at 523, 507, and 494 nm for TBA-1–TBA-3, while that of TB-1 is at 488 nm. Apparently, all these dyes show red shifted absorption maximum compared to the model compound. The result denotes that the structure changes made in TBA-1–TBA-3 could enhance the ICT process. The molar extinction coefficients (ϵ) at λ_{max} of the ICT bands for TBA-1–TBA-3 are calculated to be 3.32, 4.55, and $8.23 \times 10^4 \text{ L} \cdot \text{mol}^{-1} \cdot \text{cm}^{-1}$, respectively. Dye TBA-3 with three cyanoacrylic acid groups exhibits the highest light harvesting ability, but the smallest absorption edge of these dyes. While TBA-1 incorporating rhodanine-3-acetic acid shows the weakest light absorption ability.

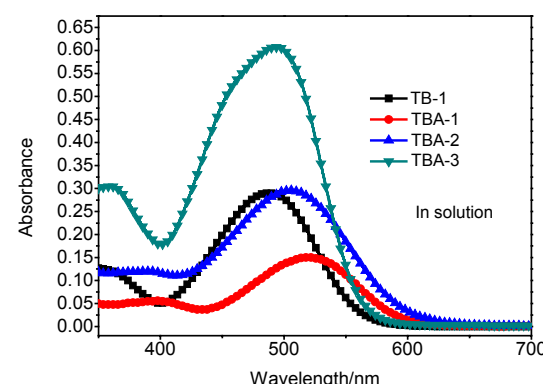


Figure 1 Absorption of bridged triphenylamine based sensitizers in chloroform (*ca.* 10⁻⁶ mol/L).

Table 1 Electrochemical and photophysical properties of TBA-1, TBA-2, TBA-3 and TB-1

Dye	$\lambda_{\text{max}}/\text{nm}^a$ [$\epsilon/(10^4 \text{ L} \cdot \text{mol}^{-1} \cdot \text{cm}^{-1})$]	$\lambda_{\text{abs}}/\text{nm}$ TiO ₂ film	E_g^{opt}/b eV	E_{HOMO}^c/c eV	E_{LUMO}^d/d eV
TBA-1	523 (3.32)	452	2.10	-4.96	-2.86
TBA-2	507 (4.55)	465	2.08	-5.15	-3.07
TBA-3	494 (8.23)	452	2.18	-5.33	-3.15
TB-1	488 (3.23)	453	2.18	-5.22	-3.04

^a Absorption spectra were measured in CH₂Cl₂ solution. ^b Calculated from $E_g^{\text{opt}} = 1240/\lambda_{\text{onset}}$. ^{c,d} E_{HOMO} was calculated by (4.74 + $E(\text{onset.ox vs. FC}^+/\text{FC})$), E_{LUMO} was calculated by $E_{\text{HOMO}} + E_g^{\text{opt}}$.

When the dyes are adsorbed onto the TiO₂ films, their absorption bands become broader. The absorption behaviors on TiO₂ are consistent with the corresponding molar extinction coefficients. Detailed photophysical data are presented in Table 1. The IPCE spectra of the

three dyes are consistent with their photophysical properties in solution. TBA-2 exhibits higher IPCE value and the more extended absorption, which is favorable for the overall performance. Dye TBA-3 still shows the strongest but a little blue-shifted absorption edge on TiO_2 . The quite poor light harvesting ability of TBA-1 may account for its low short circuit current. Notably, the absorption maxima on TiO_2 are all blue-shifted more or less as compared to that measured in chloroform (Figure 2). This could be elucidated from the H-aggregation and/or deprotonation of the carboxylic acid on TiO_2 films, according to literature report.^[29]

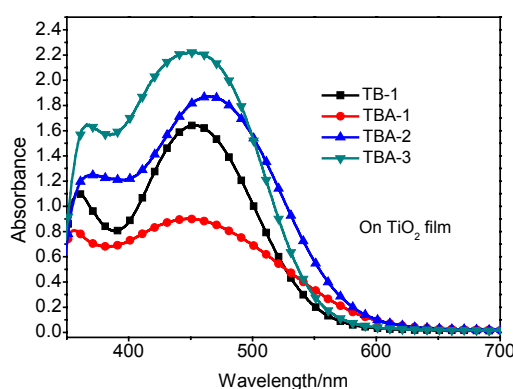


Figure 2 Absorption of bridged triphenylamine based sensitizers on TiO_2 film.

The electrochemical behaviors of these sensitizers are measured by cyclic voltammetry. The relevant CV data were presented in Table 1. The ground oxidation potentials (E_{ox}) correspond to the highest occupied molecular orbitals (HOMO). While the lowest unoccupied molecular orbitals (LUMO) were obtained from the values of E_{ox} and the band gaps (E_g^{opt}) estimated from the onset of the UV-visible absorption spectra (Table 1). The results reveal that the LUMO levels of these dyes are sufficiently higher than the conduction band edge of the TiO_2 electrode (-4.2 eV), thus providing sufficient driving force for electron injection from LUMO orbitals of these dyes to the CB band of TiO_2 . Meanwhile, the redox potential of I^-/I_3^- (-4.9 eV) is higher than the HOMO levels of TBA-2 and TBA-3, suggesting that the two dyes are able to be regenerated by the liquid electrolyte. However, the HOMO level of TBA-1 is only relatively lower than the redox potential of I^-/I_3^- , offering inefficient dye regeneration ability.

The dye structures have been analyzed by Gaussian 09 at B3LYP/6-31+G(d) level for full geometrical optimization (Figure S3).^[30] Obviously, for all of the dyes investigated, the HOMO levels are delocalized evenly throughout the entire core of the bridged TPA and the adjacent π -spacers, while the LUMO levels are mainly located on the acceptor part, and also partly on the TPA core. The molecular distribution is favorable for electronic transition from HOMO to LUMO. When these dyes are adsorbed onto the TiO_2 surface, the photoinduced electron can be effectively injected into the CB band of the semiconductor from the acceptor unit via the terminal anchoring groups. It is noteworthy that in TBA-1, the LUMO orbital is mainly located on the heterocyclic unit, but only partially distributed on the rhodanine-3-acetic acid group. This orbital distribution may lead to the inefficient electron injection from LUMO orbital of TBA-1 to the CB band of TiO_2 . On the contrary, for the dye molecules with cyanoacrylic acid acceptor (TBA-2 and TBA-3), the largely distributed LUMO on the acceptor suggests better electron injection upon photo excitation.

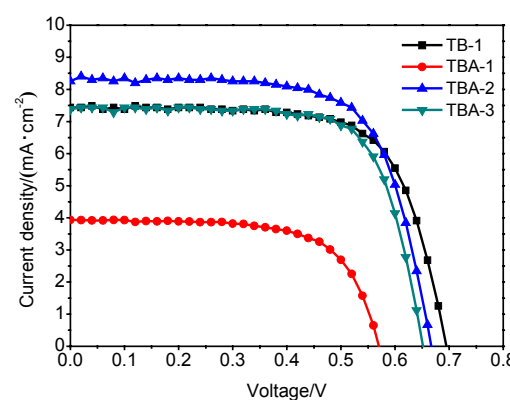


Figure 3 Photocurrent density-photovoltage curves of TB-1, TBA-2, TBA-3 and TB-1 under AM 1.5 G simulated sunlight ($100 \text{ mW}\cdot\text{cm}^{-2}$) illumination.

The typical current-voltage characteristics of DSSCs sensitized with the three dyes on TiO_2 films using I^-/I_3^- electrolyte are measured under standard AM 1.5G conditions ($100 \text{ mW}\cdot\text{cm}^{-2}$). The results are shown in Figure 3. As we have reported earlier, TB-1 showed η of 3.59%, with J_{sc} of $7.44 \text{ mA}\cdot\text{cm}^{-2}$ and V_{oc} of 694 mV. Under the same test condition, TBA-2 shows the highest power conversion efficiency of 3.87%, with a short circuit current density (J_{sc}) of $8.25 \text{ mA}\cdot\text{cm}^{-2}$, and the open circuit potential (V_{oc}) of 666 mV. TBA-4 containing three thiophene cyanoacrylic acid groups exhibits power conversion efficiency at 3.52%, with J_{sc} of $7.38 \text{ mA}\cdot\text{cm}^{-2}$ and V_{oc} of 650 mV. Compared to dye TB-1, it is obvious that the vinylthiophene spacer in TBA-2 only slightly increases the solar cell performance. Unexpectedly, three acceptor groups in TBA-4 hardly affect the J_{sc} value, but lower the V_{oc} , and therefore it exhibits slightly lower efficiency relative to TB-1. TBA-1 with rhodanine-3-acetic acid acceptor shows quite low short-circuit current of $3.94 \text{ mA}\cdot\text{cm}^{-2}$, and an open circuit voltage of 568 mV, therefore it only exhibits low power conversion efficiency of 1.5%. The above results demonstrate that the vinylthiophene linkage is favorable for dye design, while the increased acceptor groups could hardly improve the efficiency. And the rhodanine-3-acetic acid is a very poor anchoring group compared to the cyanoacrylic acid in this series of compounds. The quite poor efficiency of TBA-1 may come from its weak

light harvesting ability, the inappropriate HOMO levels, as well as the inefficient electron orbital distributions observed from their orbital geometries.

The incident photon-to-current conversion efficiencies (IPCEs) of these dyes are shown in Figure 4. The trend of IPCE values of these dyes is in accordance with their UV-Vis absorption spectra on the TiO₂ films. Similar to TB-1, TBA-2 and TBA-3 show broader IPCE spectra from 300 to 600 nm, consistent with their higher J_{sc} values.^[31] It is noteworthy that although TBA-3 shows higher IPCE spectrum than TBA-2, the weaker absorption at around 600 nm still generates lower J_{sc} in TBA-3. On the other hand, the quite low IPCE values observed from 400 to 600 nm in TBA-1 reflect lower photocurrent and hence inferior photovoltaic performance.

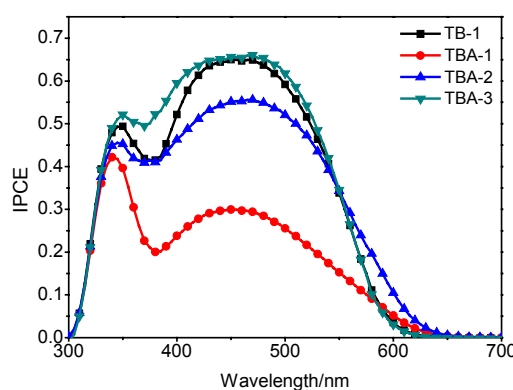


Figure 4 IPCE spectra of TBA-1, TBA-2, TBA-3 and TB-1 based devices.

Table 2 Photovoltaic performances of DSSCs based on TBA-1, TBA-2, TBA-3 and TB-1

Dye	$J_{sc}/(\text{mA} \cdot \text{cm}^{-2})$	V_{oc}/mV	Fill factor (ff)	$\eta/\%$
TBA-1	3.94	568	67.0	1.50
TBA-2	8.25	666	70.4	3.87
TBA-3	7.38	650	73.3	3.52
TB-1	7.44	694	69.7	3.59

Dye loading amounts of the dye molecules were also determined since the adsorbed sensitizers on TiO₂ films critically influence the J_{sc} . The TiO₂ film was soaked in 0.3 mmol/L organic dye in THF/ethanol (1 : 1 V/V) for 18 h in dark, and the UV-Vis absorbance of the remaining solution was measured. The dye loading of each device is then estimated from the Beer-Lambert's law with the help of the dye's respective extinction coefficient. The dye loading of each device is estimated to be $\sim 1.87 \times 10^{-7}$, $\sim 2.14 \times 10^{-7}$ and $\sim 3.46 \times 10^{-7}$ mol/cm² for TBA-1, TBA-2 and TBA-3, respectively. The relatively lower dye loading of TBA-1 may also account for its low J_{sc} value. The larger dye loading in TBA-3 may come from the firm binding ability due to the three cyanoacrylic acid groups. Whereas for TBA-2, the

moderate dye loading amount and broader absorption spectrum are favorable for the corresponding solar cell performance.

Electrochemical impedance spectroscopy (EIS) is also performed to elucidate the interfacial charge recombination processes in DSSCs based on these dyes under the dark conditions. The Nyquist plots for DSSCs based on TBA-1, TBA-2 and TBA-3 are shown in Figure 5. The larger semicircle in the lower frequency range represents the resistance of the recombination between electrons on the TiO₂ conduction band and I₃⁻ species in the electrolyte at the TiO₂/dye/electrolyte interface.^[32] The calculated resistance values (R_{rec}) are 22.35 Ω for TBA-1, 51.21 Ω for TBA-2 and 39.42 Ω for TBA-3, respectively. The larger R_{rec} demonstrates slower recombination kinetics. This trend appears to be consistent with their open circuit voltage values.

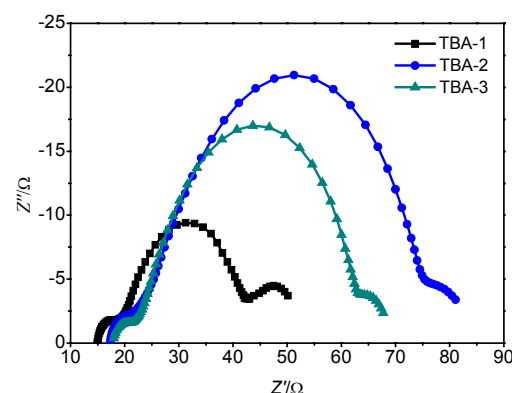


Figure 5 Nyquist plots of the DSSCs fabricated using dyes TBA-1, TBA-2 and TBA-3.

Figure 6 depicts the Bode Plots of DSSCs based on these dyes. All EIS Bode Plots exhibit two peaks featuring the frequency investigated. The one at higher frequencies corresponds to the charge transfer at the Pt/electrolyte interface and the other one at lower frequencies corresponds to the charge transfer at TiO₂/dye/electrolyte interface, which is also related to the charge recombination rate, and moreover, its reciprocal is asso-

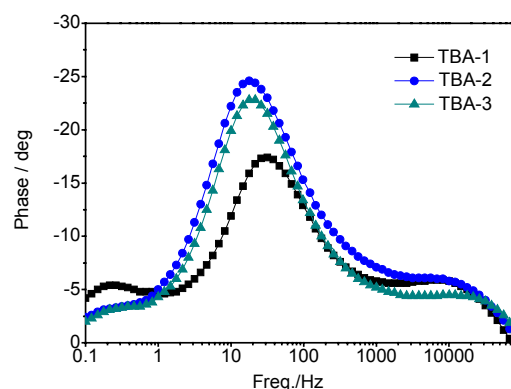


Figure 6 Bode-phase plots of the DSSCs fabricated using dyes TBA-1, TBA-2 and TBA-3.

ciated with the electron lifetime.^[33] The electron lifetime (τ) was estimated to be in the order of TBA-2>TBA-3>TBA-1, which is also in good agreement with their open circuit voltage results.

Conclusions

In summary, we have demonstrated the design and synthesis of new D- π -A type organic sensitizers containing bridged triphenylamine groups. Dye TB-1 was also studied as the reference compound. Their photo-physical properties were studied and the photovoltaic applications as sensitizers were investigated. Moreover, the effects of various acceptors, as well as vinylthiophene linkage were evaluated. Compared to TB-1, the introduction of vinylthiophene linkage in TBA-2 resulted in broadened absorption and IPCE spectra. In addition, the EIS experiments suggest larger R_{rec} and longer electron lifetime of TBA-2. Therefore, it outperforms the other dyes, exhibiting the highest power conversion efficiency of 3.87%, with J_{sc} of 8.25 mA•cm⁻² and V_{oc} of 666 mV under simulated AM 1.5 irradiation (100 mW•cm⁻²). Whereas, TBA-3 with three acceptor groups only shows efficiency of 3.52%, indicating the increased acceptor groups have little effect on performance. In contrast, the quite poor efficiency of TBA-1 should be associated with its weak light harvesting ability, the inappropriate HOMO levels, as well as the inefficient electron injection ability observed from its orbital geometries.

Acknowledgement

This work is financially supported by the National Natural Science Foundation of China (No. 51203046), and the “Fundamental Research Funds for the Central Universities” (XDKJ2014C145 and XDKJ2014C052), as well as the Starting foundation of Southwest University (Nos. SWU113076 and SWU113078).

References

- [1] O'Regan, B.; Grätzel, M. *Nature* **1991**, *353*, 737.
- [2] Chung, I.; Lee, B.; He, J.; Chang, R. P. H.; Kanatzidis, M. G. *Nature* **2012**, *485*, 486.
- [3] Hagfeldt, A.; Boschloo, G.; Sun, L.; Kloo, L.; Pettersson, H. *Chem. Rev.* **2010**, *110*, 6595.
- [4] (a) Wang, L.; Yang, X.; Wang, X.; Sun, L. *Dyes Pigments* **2015**, *113*, 581; (b) Wang, Z.; Xu, H.; Zhang, Z.; Zhou, X.; Pang, S.; Cui, G. *Chin. J. Chem.* **2014**, *32*, 491; (c) Ma, Y.; Wang, S.; Zheng, L.; Lu, Z.; Zhang, D.; Bian, Z.; Huang, C.; Xiao, L. *Chin. J. Chem.* **2014**, *32*, 957; (d) Jia, Y.; Gou, F.; Fang, R.; Jing, H.; Zhu, Z. *Chin. J. Chem.* **2014**, *32*, 513; (e) Wu, W.; Zhang, X.; Hu, Y.; Jin, B.; Hua, J. *Chin. J. Chem.* **2013**, *31*, 388; (f) Wei, Y.; Wu, Z.; An, Z.; Chen, X.; Chen, P.; Liu, Q. *Chin. J. Chem.* **2014**, *32*, 474.
- [5] Nazeeruddin, M. K.; Péchy, P.; Renouard, T.; Zakeeruddin, S. M.; Humphry-Baker, R.; Comte, P.; Liska, P.; Cevey, L.; Costa, E.; Shklover, V.; Spiccia, L.; Deacon, G. B.; Bignozzi, C. A.; Grätzel, M. *J. Am. Chem. Soc.* **2001**, *123*, 1613.
- [6] Yella, A.; Lee, H. W.; Tsao, H. N.; Yi, C.; Chandiran, A. K.; Nazeeruddin, M. K.; Diau, E. W. G.; Yeh, C. Y.; Zakeeruddin, S. M.; Grätzel, M. *Science* **2011**, *334*, 629.
- [7] Chae, Y.; Kim, S. J.; Kim, J. H.; Kim, E. *Dyes Pigments* **2015**, *113*, 378.
- [8] Stalder, R.; Xie, D.; Islam, A.; Han, L.; Reynolds, J. R.; Schanze, K. S. *ACS Appl. Mater. Interfaces* **2014**, *6*, 8715.
- [9] (a) Liang, M.; Chen, J. *Chem. Soc. Rev.* **2013**, *42*, 3453; (b) Gu, C. Z.; Meng, S. X.; Feng, Y. Q. *Chin. J. Org. Chem.* **2015**, DOI: 10.6023/cjoc201412018; (c) Kou, D.; Liu, W.; Hu, L.; Chen, S.; Huang, Y.; Dai, S. *Acta Chim. Sinica* **2013**, *71*, 777; (d) Kou, D.; Liu, W.; Hu, L.; Chen, S.; Huang, Y.; Dai, S. *Acta Chim. Sinica* **2013**, *71*, 1149; (e) Xiong, B.; Zhu, Z.; Wang, C.; Chen, B.; Luo, J. *Acta Chim. Sinica* **2013**, *71*, 443; (f) Tang, X.; Wang, Y. *Acta Chim. Sinica* **2013**, *71*, 193.
- [10] Yan, K.; Lu, X.; Qiu, Y.; Liu, Z.; Sun, J.; Yan, F.; Guo, W.; Yang, S. *Org. Lett.* **2012**, *14*, 2214.
- [11] (a) Cai, S.; Tian, G.; Li, X.; Su, J.; Tian, H. *J. Mater. Chem. A* **2013**, *1*, 11295; (b) Cai, S.; Hu, X.; Zhang, Z.; Su, J.; Li, X.; Islam, A.; Han, L.; Tian, H. *J. Mater. Chem. A* **2013**, *1*, 4763; (c) Ning, Z.; Tian, H. *Chem. Commun.* **2009**, 5483; (d) Kouruma, N.; Wang, Z.-S.; Mori, S.; Miyashita, M.; Suzuki, E.; Hara, K. *J. Am. Chem. Soc.* **2006**, *128*, 14256.
- [12] Im, H.; Kim, S.; Park, C.; Jang, S. H.; Kim, C. J.; Kim, K.; Park, N. G.; Kim, C. *Chem. Commun.* **2010**, 1335.
- [13] Liu, W. H.; Wu, I. C.; Lai, C. H.; Lai, C. H.; Chou, P. T.; Li, Y. T.; Chen, C. L.; Hsu, Y. Y.; Chi, Y. *Chem. Commun.* **2008**, 5152.
- [14] Haid, S.; Marszalek, M.; Mishra, A.; Wielopolski, M.; Teuscher, J.; Moser, J. E. *Adv. Funct. Mater.* **2012**, *22*, 1291.
- [15] Tan, L. L.; Chen, H. Y.; Hao, L. F.; Shen, Y.; Xiao, L. M.; Liu, J. M.; Kuang, D. B.; Su, C. Y. *Phys. Chem. Chem. Phys.* **2013**, *15*, 11909.
- [16] (a) Liang, M.; Xu, W.; Cai, F.; Chen, P.; Peng, B.; Chen, J.; Li, Z. J. *Phys. Chem. C* **2007**, *111*, 4465; (b) Xu, W.; Peng, B.; Chen, J.; Liang, M.; Cai, F. *J. Phys. Chem. C* **2008**, *112*, 874; (c) Lee, D. H.; Lee, M. J.; Song, H. M.; Song, B. J.; Seo, K. D.; Pastore, M.; Anselmi, C.; Fantacci, S.; De Angelis, F.; Nazeeruddin, M. K. *Dyes Pigments* **2011**, *91*, 192.
- [17] Hagberg, D. P.; Yum, J. H.; Lee, H.; De Angelis, F.; Marinado, T.; Karlsson, K. M.; Humphry-Baker, R.; Sun, L.; Hagfeldt, A.; Grätzel, M.; Nazeeruddin, M. K. *J. Am. Chem. Soc.* **2008**, *130*, 6259.
- [18] Fang, Z.; Teo, T. L.; Cai, L. P.; Lai, Y. H.; Samoc, A.; Samoc, M. *Org. Lett.* **2009**, *11*, 1.
- [19] Jiang, Z.; Ye, T.; Yang, C.; Yang, D.; Zhu, M.; Zhong, C.; Qin, J.; Ma, D. *Chem. Mater.* **2011**, *23*, 771.
- [20] Field, J. E.; Venkataraman, D. *Chem. Mater.* **2002**, *14*, 962.
- [21] Jiang, Z.; Chen, Y.; Yang, C.; Cao, Y.; Tao, Y.; Qin, J.; Ma, D. *Org. Lett.* **2009**, *11*, 1503.
- [22] Cai, L.; Tsao, H. N.; Zhang, W.; Wang, L.; Xue, Z.; Grätzel, M.; Liu, B. *Adv. Energy Mater.* **2012**, *3*, 200.
- [23] Do, K.; Kim, D.; Cho, N.; Paek, S.; Song, K.; Ko, J. *Org. Lett.* **2012**, *14*, 222.
- [24] Wu, F.; Zhao, S.; Lee, L.; Wang, M.; Chen, T.; Zhu, L. *Tetrahedron Lett.* **2015**, DOI: 10.1016/j.tetlet.2015.01.156.
- [25] Emilio, A.; Carmen, N. *J. Org. Chem.* **2009**, *74*, 2321.
- [26] Zhu, L. N.; Yang, H. B.; Zhong, C.; Li, C. M. *Dyes Pigments* **2014**, *105*, 97.
- [27] Cheng, M.; Yang, X.; Chen, C.; Zhao, J.; Tang, Q.; Sun, L. *Phys. Chem. Chem. Phys.* **2013**, *15*, 17452.
- [28] Hua, Y.; Chang, S.; Huang, D.; Zhou, X.; Zhu, X.; Zhao, J.; Chen, T.; Wong, W. Y.; Wong, W. K. *Chem. Mater.* **2013**, *25*, 2146.
- [29] Lin, L. Y.; Tsai, C. H.; Wong, K. T.; Huang, T. W.; Hsieh, L.; Liu, S. H.; Lin, H. W.; Wu, C. C.; Chou, S. H.; Chen, S. H.; Tsai, A. I. *J. Org. Chem.* **2010**, *75*, 4778.
- [30] Frisch, M. J.; Trucks, G. W.; Schlegel, H. B.; Scuseria, G. E.; Robb, M. A.; Cheeseman, J. R.; Scalmani, G.; Barone, V.; Mennucci, B.; Petersson, G. A.; Nakatsuji, H.; Caricato, M.; Li, X.; Hratchian, H. P.; Izmaylov, A. F.; Bloino, J.; Zheng, G.; Sonnenberg, J. L.; Hada,

M.; Ehara, M.; Toyota, K.; Fukuda, R.; Hasegawa, J.; Ishida, M.; Nakajima, T.; Honda, Y.; Kitao, O.; Nakai, H.; Vreven, T.; Montgomery, Jr., J. A.; Peralta, J. E.; Ogliaro, F.; Bearpark, M.; Heyd, J. J.; Brothers, E.; Kudin, K. N.; Staroverov, V. N.; Kobayashi, R.; Normand, J.; Raghavachari, K.; Rendell, A.; Burant, J. C.; Iyengar, S. S.; Tomasi, J.; Cossi, M.; Rega, N.; Millam, N. J.; Klene, M.; Knox, J. E.; Cross, J. B.; Bakken, V.; Adamo, C.; Jaramillo, J.; Gomperts, R.; Stratmann, R. E.; Yazev, O.; Austin, A. J.; Cammi, R.; Pomelli, C.; Ochterski, J. W.; Martin, R. L.; Morokuma, K.; Zakrzewski, V. G.; Voth, G. A.; Salvador, P.; Dannenberg, J. J.;

Dapprich, S.; Daniels, A. D.; Farkas, Ö.; Foresman, J. B.; Ortiz, J. V.; Cioslowski, J.; Fox, D. J. *Gaussian 09*, Revision A.02, Gaussian, Inc., Wallingford CT, 2009.

- [31] Qian, X.; Zhu, Y. Z.; Song, J.; Gao, X. P.; Zheng, J. Y. *Org. Lett.* **2013**, *15*, 6034.
[32] He, J. J.; Benko, G.; Korodi, F.; Polivka, T.; Lomoth, R.; Akermark, B.; Sun, L. C.; Hagfeldt, A.; Sundstrom, V. *J. Am. Chem. Soc.* **2002**, *124*, 4922.
[33] van de Lagemaat, J.; Park, N. G.; Frank, A. J. *J. Phys. Chem. B* **2000**, *104*, 2044.

(Pan, B.; Qin, X.)